Operational water forecast ability of the iSnobal-HRRR coupling; an evaluation to adapt into production environments

Joachim Meyer[1], S. McKenzie Skiles[1], John Horel[2], Patrick Kormos[3], Andrew Hedrick[4], Ernesto Trujillo[5,4]

[1] Department of Geography, University of Utah, Salt Lake City, UT, USA
5   [2] Department of Atmospheric Sciences, University of Utah, Salt Lake City, UT, USA
[3] Colorado Basin River Forecast Center NOAA National Weather Service, Salt Lake City, UT, USA
[4] Northwest Watershed Research Center, USDA Agricultural Research Service, Boise, ID, USA
[5] Department of Geosciences, Boise State University, Boise, ID, USA

Correspondence to: Joachim Meyer (j.meyer@utah.edu)

10   **Abstract**

Operational water-resource forecasters, such as the Colorado Basin River Forecast Center (CBRFC) in the Western United States rely on historical records to calibrate the temperature-index models currently used for snowmelt runoff predictions. This data dependence is increasingly challenged, with global and regional climatological factors changing the seasonal snowpack in mountain watersheds. To evaluate and improve the CBRFC modeling options, this work ran the physically based snow energy

15   balance iSnobal model, forced with outputs from the High-Resolution Rapid Refresh (HRRR) numerical weather model across four years in a subset region. Compared to in-situ, remotely sensed, and the current operational CBRFC model, the iSnobal-HRRR coupling showed well-reconstructed snow depths until peak accumulation (Mean differences between -0.20 and +0.28 m). Once snowmelt set in, iSnobal-HRRR showed that simulated snowmelt was slower relative to observations, depleting snow on average up to 34 days later. The melting period is a critical component for water forecasting. Based on the results, there is a need for revised

20   energy balance calculations in iSnobal, which is a recommended future improvement to the model. Nevertheless, the presented performance and architecture make iSnobal-HRRR a promising combination for the CBRFC production needs, where there is a demonstrated change to the seasonal snow in the mountain ranges around the Colorado River Basin. Long term goal is to introduce the iSnobal-HRRR coupling in day-to-day CBRFC operations, and this work created the foundation to expand and evaluate larger domains.

1. Introduction

Freshwater supply, originating as melt from seasonal snowpack runoff, has experienced a shift in timing and magnitude in recent decades (Mote et al., 2018; Stewart, 2009). Higher observed temperatures during the winter (Musselman et al., 2021), for instance, lead to precipitation phase changes resulting in more precipitation as rain over snow in low elevation areas (Feng and Hu, 2007; Knowles et al., 2006). The magnitude of the changes varies regionally (Harpold et al., 2012; Skiles and Painter, 2017) increasing the complexity of understanding and forecasting impacts Changing snowpack trends are expected to continue, as evidenced by simulations with predicted future climate conditions (Cho et al., 2021; Ikeda et al., 2021; Li et al., 2017; Musselman et al., 2017). This presents a challenge from a modeling perspective, especially in operational settings. A consistent and accurate estimate of snowpack runoff is getting harder with the increasingly different snow accumulation, snow melt, and snow cover extents across the seasonally snow-covered mountain ranges supplying freshwater to the downstream regions.

Presently, a subset of the hydrologic forecast agencies in the United States use temperature-index models, such as SNOW-17 (Anderson 1976), which have historically performed well in operational settings while requiring few meteorological observations (Franz et al., 2008). In principle, SNOW-17 calculates the snowmelt using the correlation between air temperature and available melt energy from net solar radiation and a calibration factor, which increases as the melt period progresses (Anderson, 1976; Franz et al., 2010). The best model predictions are with domain-specific calibration parameters from historical data with the modeled year following the snow accumulation and melt conditions from the past (He et al., 2011). Once conditions depart from the historical average, such as lower snow albedo from highly variable inter-annual dust deposition events (Bryant et al., 2013), the SNOW-17 model forecast errors increase and requires significant forecaster interaction to account for the variable conditions. One effort to improve the accuracy of SNOW-17 applied the Bayesian Model Averaging method across an ensemble of twelve snow models, each consisting of different components from SNOW-17 (Franz et al., 2010). Although the results improved compared to running SNOW-17 as a standalone application, the setup was only tested at the 1d point scale and required different weights for the individual models between test locations. This increased complexity makes the method challenging to apply across larger spatial scales in daily operations. Ultimately, temperature-index models cannot adapt to rapidly changing snow accumulation and melt conditions without adding more meteorological inputs, and the long-term historical records (30 to 40 years) are becoming less representative to calibrate the model parameters.

One option to improve forecasting results is the use of physically based models that incorporate more meteorological measurements. Physically based modeling is also referred to as 'energy-balance' or 'process-based' in the literature, and in the context of this work, we will use 'physically based'. In general, physically based models use weather observations such as relative humidity, wind speeds, and radiation, among others, to resolve the mass and energy balances of the snowpack, which determines the snowmelt rate and meltwater runoff (Marks and Dozier, 1992). Although there are several physically based snow models (e.g., CROCUS, Brun, et al., 1989; Factorial Snow Model, Essery, 2015; SNOWPACK, Lehning et al., 2002; SnowModel, Liston and Elder, 2006), this work focused on iSnobal. Initially, iSnobal (Snobal for the point version) was developed as a two-layer snowpack model (Marks and Dozier, 1992; Marks et al., 1992) and evolved later to a spatially distributed version (Marks et al., 1999), maintaining the point-level architecture and relatively simple input data requirements. A recent addition to the modeling pipeline is the Spatial Modeling for Resource Framework (SMRF, Havens et al., 2017), which assists in distributing the forcing data across the model domain. To streamline the workflow and increase reproducibility, the Automated Water Supply Model (AWSM) integrated iSnobal and SMRF into a central execution environment (Havens et al., 2020). To this date, iSnobal has been successfully deployed to simulate snowpacks in watersheds sizes from less than 1 km^2 to over 1000 km^2 (Garen and Marks, 2005; Hedrick et al., 2018, 2020; Kormos et al., 2014).

The increased meteorological measurement requirements to calculate the mass and energy balances of physically based models
65 cannot always be satisfied by in-situ observation networks. Where instrumentation sites are present in the modeled domain, the available observations are not guaranteed to provide all required model inputs such as wind speed or radiation, can have data gaps through time, or do not satisfy the necessary data quality. An alternative to in-situ stations is using outputs from numerical weather prediction (NWP) models, which are generally spatially and temporally complete and provide all the required forcing variables from a single source. The adaptation of NWP model output to provide forcing data for snow models is ongoing and has been
70 successfully tested as a standalone source for point simulations (Bellaire et al., 2011, 2013; Iwamoto et al., 2008) or spatially in combination with data assimilation and filtering techniques (Griessinger et al., 2019; Vernay et al., 2021). Adding NWP as a possible weather measurement input source to iSnobal was first evaluated in (Havens et al., 2019), where downscaled and bias-corrected observations from Weather Research and Forecasting (WRF) Model had the best results. A follow-up effort to the WRF integration into iSnobal also added support for the High-Resolution Rapid Refresh (HRRR) model (Benjamin et al., 2016) from
75 the National Oceanic and Atmospheric Administration (NOAA). HRRR assimilates available radar observations every hour and produces forecasts up to 18-hours in advance at the 3 km spatial resolution. The HRRR model has been under active development since it became the United States National Weather Service's (NWS) operational forecast model in late 2014 (Bytheway et al., 2017) and is currently in its fourth iteration. The HRRR data are publicly available via different providers (Google Cloud Platform, Amazon Web Services, NOAA) and are readily integrable for research and operational purposes (Gowan et al., 2022).
80 Among the many regions impacted by the changing seasonal snow and environmental conditions around the globe (Ayers et al., 2016; Cho et al., 2021; Christensen and Lettenmaier, 2007; Dettinger et al., 2015) is the Western United States of America, where 53% to 70% of the annual freshwater supply originates from seasonal snowmelt (Li et al., 2017). For example, the Colorado River Basin (CRB), with its headwaters located in the Rocky Mountains, is currently trending towards a shorter duration and reduced extent of snow cover in the winter based on in-situ measurements from 1984 to 2009 (Harpold et al., 2012) and earlier dates for
85 maximum snow water equivalent (SWE) compared to long-term historical records (Musselman et al., 2021). The CRB region also has an increase in snow darkening following the deposition of light-absorbing particles (Skiles and Painter, 2017; Skiles et al., 2012), which accelerates snowmelt timing and magnitude (Painter et al., 2018). Freshwater supply forecasting in this region is done by the Colorado Basin River Forecast Center (CBRFC), part of the National Weather Service (NWS) in the United States of America. The CBRFC uses SNOW-17 as part of their operational water availability forecasting model and faces increased
90 challenges in adapting to the observed and predicted seasonal snow changes. The underlying long-term historical calibration records from the CBRFC do not fully account for climate variability and will continue to be less representative in the future. Capturing the different timing and magnitudes of snowmelt requires new methods.

In this paper, the iSnobal-HRRR coupling is documented and described for the first time and assessed across four water years (2018 – 2021) in the East River Watershed, Colorado, USA. The model evaluation was in collaboration with the CBRFC to gauge
95 the feasibility of supplementing SNOW-17 with a physically based model. Physically based models have been identified by the United States Bureau of Reclamation as an underutilized emerging technology for snow measurements, and iSnobal was evaluated as a "flight qualified" product through tests and demonstration (The Bureau of Reclamation, 2022). In contrast to the current literature evaluating iSnobal in operational environments, this work focuses on HRRR as a standalone forcing input source without bias corrections (Havens et al., 2019) or updates from spatial observations (Hedrick et al., 2018, 2020). Removing input data
100 corrections or model updates through in-situ observations increases the CBRFC's ability to adapt the workflow into their daily operations and speeds up model preparation and execution times. For the overall iSnobal model assessment, the simulated snow depth was compared against measured observations at discrete in-situ snow measurement stations and spatially at discrete points in time against aerial snow depth maps. The iSnobal simulated runoff was compared to the basin hydrograph for basin-averaged

assessment. Finally, iSnobal-HRRR precipitation inputs and SWE outputs were compared to SNOW-17 to assess the differences

105   between the models. This work is an effort to support the increased inclusion of physically based models in operational water supply forecasting in snow-dominated environments. Broadly, this work also contributes to the NWS Advanced Hydrologic Prediction Service program operational goals (Council, 2006) by aiming to make hydrological forecasting more accurate and resilient in the face of change.

2. Study Area

110   The East River Watershed (ERW) is a high alpine watershed located in the Upper Gunnison River Basin, part of the Colorado River Basin. The East River is one of two primary tributaries of the Gunnison River, which discharges downstream into the Colorado River (Figure 1). A stream gauge station at an elevation of 2440 m near Almont, CO is operated by the United States Geological Survey (USGS) and monitors the streamflow of the East River year-round. This station is the central discharge point for seasonal snow runoff in the watershed. The ERW has representative characteristics for mountain watersheds in Colorado with

115   an average elevation of 3266 m, high vertical elevation relief (1420 m; Hubbard et al., 2018), and a mixture of different vegetation types (bush and grassland or mixed conifer and aspen trees).

There are three Snow Telemetry (SNOTEL) stations that are operated by the United States Department of Agriculture National Resource Conservation Service (USDA-NRCS) in the modeled domain: Schofield Pass (elevation: 3261 m), Butte (elevation: 3097 m), and Upper Taylor (elevation: 3243 m). The Upper Taylor station does not sit within the ERW boundaries but was included in

120   this study to expand the number of available in-situ comparison sites within the model domain. The CBRFC divides the ERW into three topographical hydrologic response units (HRU); lower, middle, and upper (Figure 1). Each HRU is based on elevation and are modeled independent from each other (Council, 2006). The division will be used in this work to refer to the respected spatial area.
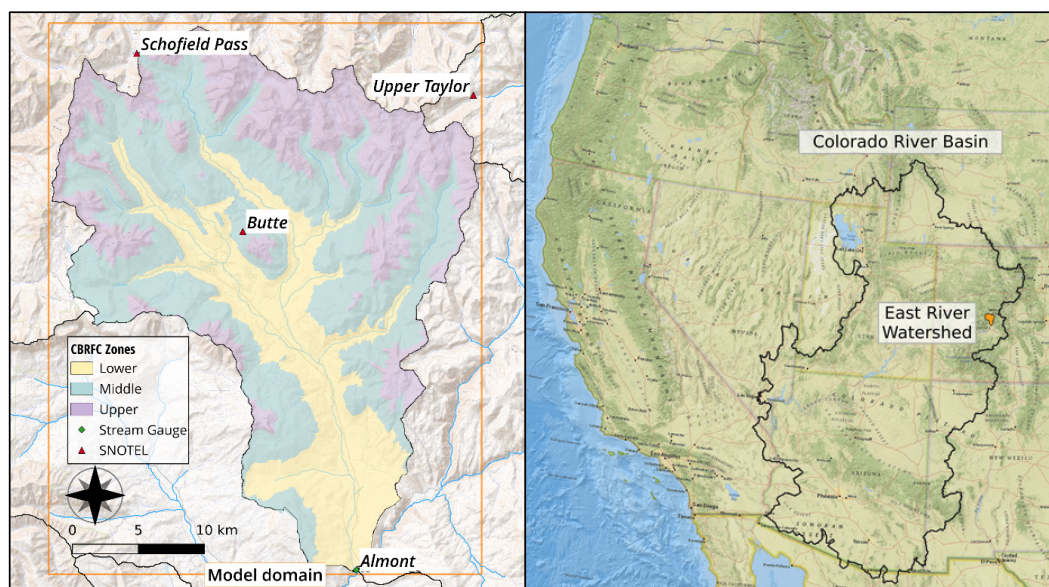
Figure 1 – Overview of the East River Watershed (black boundaries) and iSnobal modal domain (orange outline) are shown on the left. There are three SNOTEL sites along with the stream gauge station. The watershed is divided into three HRUs by the CBRFC. The location of the watershed and area of the Colorado River Basin is shown on the right. Basemap (right): © ESRI

3. Model Setup

3.1 Model Description

125   Using temporally complete meteorological input data, the iSnobal model simulates snowpack evolution by solving energy and mass balance fluxes. As a two-layer model, the top layer is designated for all energy and mass exchanges between the snow surface and the atmosphere. The bottom layer acts as an interface for mass and energy exchanges between the top and soil layers. Once the net energy fluxes of the two snowpack layers exceed the cold content (the energy required to raise the entire snowpack to 0 ˚C

130   temperature) and the snow meltwater amount exceeds the maximum liquid water holding capacity of the snowpack, the water outflow at the base of the snowpack is calculated (i.e., surface water input (SWI) hereinafter).

The required forcing input data to calculate energy and mass balance fluxes include air temperature, relative humidity, incoming solar radiation, wind speed and direction, and total precipitation. These may originate from distributed point measurements or gridded data (e.g., NWP models). Before calculating the fluxes, the input data are spatially interpolated and distributed for the

135   model domain in SMRF, which also solves for additional essential variables for the energy balance calculations in iSnobal. For instance, net solar radiation, a function of incoming shortwave radiation and snow albedo is resolved internally in SMRF. A detailed description of the energy balance equations and data preparation can be found in Marks et al. (1992), Marks et al. (1999), Link et al. (2004), and Havens et al. (2017; 2020). All energy and mass balance calculations in iSnobal are based on a fixed spatial grid and a configurable time interval. The main driver for the chosen time interval to update the snowpack conditions is the temporal

140   resolution of the input data, which needs to be fine enough to resolve diurnal climatic variations (e.g., temperature or solar radiation).

3.2 Software Architecture

A complete installation of the iSnobal model requires several components and are available as open-source software. All components were written and are maintained by the United States Department of Agriculture, Agriculture Research Service

145   (USDA-ARS) in Boise, ID, USA, and downloadable as Docker containers or installable from source via GitHub (https://github.com). Before executing iSnobal, the model domain is set up and requires collecting the domain information such as elevation data, output resolution, and vegetation data. This step is a one-time process, not repeated between simulation years, and assisted by the Basin Setup tool (https://github.com/USDA-ARS-NWRC/basin_setup).

Once the model domain setup is completed, the model itself needs to be installed. The main components necessary to run iSnobal

150   are Katana (https://github.com/USDA-ARS-NWRC/katana), SMRF (https://github.com/USDA-ARS-NWRC/smrf), and the Automated Water Supply Model (AWSM, https://github.com/USDA-ARS-NWRC/awsm). Katana is a pre-processing module that uses the WindNinja model (Forthofer 2014) to downscale the HRRR wind data to the model resolution (e.g., 3 km to 50 m). WindNinja, initially designed for wildfire applications, simulates

155   wind speeds at high spatial resolutions over complex topography. AWSM automates the execution of SMRF and iSnobal for each time step and acts as overarching control software. AWSM and SMRF are additionally available as installable and documented Python packages. An overview of the architecture and workflow,

160   including the data in- and outflow, is visualized in Figure 2 and is fully described in Havens et al. (2020).
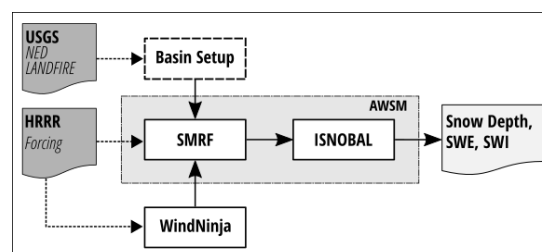
Figure 2 – Overview of the iSnobal model architecture, including the input data to setup the model domain and forcing data to run an individual day. At the end of an iteration, the end of day values are stored as individual outputs.

3.3 Compute Environment

The computational resources required for running the model in this work were provided by the Center for High Performance
Computing at the University of Utah. All model components were installed from source, with the exception for Katana, where the
165 containerized option was selected due to the complexity of dependent libraries. The installation was documented and published on
GitHub (https://github.com/UofU-Cryosphere/isnoda) and extends the official documentation for each component with
instructions for a shared compute environment and helper scripts for data download and model execution.

3.4 Numerical Weather Prediction Inputs

The meteorological inputs required to run the model were retrieved from the sixth-hour HRRR forecast product. HRRR is
170 undergoing active development, and the water years simulated in this study used the product versions HRRRv2 (October 2017 to
July 2018), HRRRv3 (July 2018 to November 2020), and HRRRv4 (December 2020 to August 2021). Using the sixth-hour HRRR
forecast allows for better utilization of model physics along with the assimilated observations (Bytheway et al., 2017) and is a
common practice for other NWP input products (Schirmer and Jamieson, 2015). Refinements to the HRRR data include upscaling
the vertical and horizontal wind data to 200 m resolution by Katana using the model domain topographic data. Another input to
175 note is incoming solar radiation. The current SMRF implementation only uses this HRRR variable to determine the cloud factor.
The required incoming solar radiation input used in iSnobal is calculated by SMRF from the typographically adjusted incoming
clear sky radiation of the model domain (Dozier 1990) and scaled by the cloud factor.

3.5 East River Watershed Model Domain Setup and Execution

The iSnobal model was prepared to run at a 50 m spatial resolution over the study area, resulting in 837 x 656 grid cells and an
180 area of 1373 km². This spatial resolution followed the recommendations of Winstral et al. (2014), which found that for basin-scale
modeling studies, a resolution between 25 m and 100 m resolves local processes in heterogeneous mountain environments without
requiring the longer computation time of higher resolutions. The ERW basin setup used elevation data from the National Elevation
Dataset by the USGS and vegetation data from the USGS through the LANDFIRE spatial products. Both data sources are publicly
available and distributed through the USGS.
185 Snowpack mass and energy fluxes were simulated with iSnobal from 2018 through 2021 in one-hour time steps, matching the
HRRR temporal resolution. The model was configured to store the end-of-day values, matching the temporal resolution of the
available in-situ comparison observations and the SNOW-17 inputs and outputs, which are further explained in the model
comparison section. A single model year was initiated on the 1st of October and ended on the 30th of September. This date range
is a 'water year' and a standard definition for hydrologic forecasting in the United States, defined by the USGS.

190 ### 4 Model Comparison

Two types of measurements were used to compare selected iSnobal outputs with reference values: discrete in-situ time-series
measurements and spatially distributed snapshots at a single point in time. The in-situ observations were the quality-controlled
end-of-day values for snow depth measurements from the three SNOTEL stations. This assessment against the SNOTEL data used
a spatial maximum and minimum of a 2x2 grid surrounding the point location of the sites (Figure 3). This approach was based on
195 visual inspections of the locations. Each site showed an offset to the center of the model output cell, and a spatial grid was deemed
more appropriate to account for the physiographic variability surrounding their location. For the years with available ASO spatial
observations (2018 to 2020), simulated snow depths were compared to the ASO lidar snow depths. The range of snow depth values

on ASO flight days was also included in the time-series comparison and used the same 2x2 grid surrounding the SNOTEL sites (Figure 3).

200   The spatial point in time comparison used lidar-based snow depth maps from the Airborne Snow Observatory (ASO, Painter, et al., 2016), which surveyed the area twice in 2018 and 2019 and once in 2020. In 2018 and 2019, the first survey happened during the snow accumulation season, and the second survey happened after peak SWE during snowmelt progression. In 2020, the area was

205   surveyed before peak SWE. The spatial resolution of the ASO snow depth maps matched the iSnobal model resolution of 50 m, and the spatial extent overlapped with the ERW boundaries. Across the years, the ASO snow depth maps were used as the reference, and the model simulated snow depth was subtracted from the lidar snow depth on a pixel-by-pixel basis. The goal of this

Figure 3 – SNOTEL site location relative to configured model output resolution of 50 m (green dashed grid). No site was centered in one pixel and a spatial 2x2 grid surrounding the site was used for simulated iSnobal comparison values. Basemap: © ESRI

210   comparison was to check for any spatial biases in simulated snow depths across elevation bands or aspects and for different snow conditions (accumulating or melting) in years with two flights (2018 and 2019). To assess how well the iSnobal simulated melt aligned with the ERW snowmelt-dominated hydrograph, all SWI of the model grid cells in the watershed boundaries were summed up and compared against the stream gauge at the basin pour point. This comparison used a seven-day moving average window to reduce daily spikes in the time series. The focus of this evaluation was on timing and

215   magnitude; in a basin like ERW, the simulated SWI should follow the temporal pattern measured at the stream gauge, which is influenced by the snowmelt runoff. Finally, to better understand how iSnobal-HRRR compares to SNOW-17 for operational forecasting, the precipitation inputs and SWE outputs from both models were compared. The gridded iSnobal data was summarized by HRU (Figure 1) and individually compared to the SNOW-17 input/output data provided by the CBRFC. Mean areal precipitation values by the CBRFC originate from precipitation measurement stations in and around ERW, are quality controlled, and combined

220   using a weighting equation derived during calibration with the primary target being PRISM (Parameter elevation Regression on Independent Slopes Model) statistical mapping grids. Neither of these datasets are considered the true values; rather, this model inter-comparison was undertaken to understand how (and why) the models may differ. Additionally, iSnobal simulated snow depths were compared to ASO lidar snow depths in each HRU.

5. Results

225   ### 5.1 Run time

Running the model through an entire water year took around eighteen hours in total, with WindNinja taking one-third of the time, and AWSM accounting for the remaining 12 hours. The compute times are based on a machine with 24 processor cores, 24 GBs of RAM, and hyper-threading enabled, which increased the number of processing threads to 48. The storage requirement for the input data was 10 GBs, with the model output occupying another 100 GBs of space. Iterating from one day to the next took less

230   than five minutes, including data download, pre-processing, and running the model. This reasonably fast execution and total storage requirement showed that the model could be implemented in day-to-day operations.

5.2 SNOTEL comparison

Across all simulated years, there was a good agreement during the accumulation period between simulated iSnobal and observed SNOTEL snow depths. For the two sites within the ERW watershed boundaries (Butte and Schofield Pass), the simulated depths
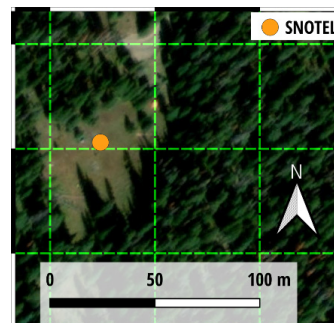
235   had a mean difference between +0.28 m and -0.20 m until peak SWE (Supplement Figure S2), while the Upper Taylor site had consistently higher than observed snow depth (Mean difference between -0.17 m and -0.53 m; Supplement Figure S2). This site-specific observation was consistent across all comparison years and not affected by annual differences in the accumulation magnitudes. An example of an average snow depth year (2018) and an above-average year (2019) is shown in Figure 4. Additional figures for 2020 and 2021 can be found in the Supplement Figure S1 to this paper.

240   For the early season ASO flights in 2018, iSnobal had higher snow depths around the Butte (Mean difference (MD) +0.35 m) and Schofield Pass (MD +0.20 m) SNOTEL sites compared to the ASO values. The SNOTEL measured differences on the flight days were close at the Butte (Difference +0.10 m to +0.13 m) and the Schofield Pass (+0.04 m to +0.08m) site. The late-season flight, where snow was still present at the Schofield Pass site, had the iSnobal snow depths closer in line with ASO (MD -0.07 m) and was above the SNOTEL (+0.20 m to +0.54 m). For 2019, the early season ASO-iSnobal snow depth differences across SNOTEL

245   locations varied with higher iSnobal values at Butte (MD +0.25 m) and Upper Taylor (MD +0.39 m) and lower at Schofield Pass (MD -0.22 m). The flight day differences to measured SNOTEL values were almost identical at Butte (0.00 m to 0.04 m), negative at Schofield Pass (-0.32 m to -0.43 m), and positive Upper Taylor (+0.16 m to +0.61 m). The late-season snow depths in 2019 overlapped at Butte between ASO-iSnobal (MD +0.19 m) with no snow measured by SNOTEL, while Schofield Pass had iSnobal lower than ASO (MD -0.31 m) and overlap with SNOTEL measured (+0.11 m to -0.66 m). The Upper Taylor site had iSnobal

250   much higher than ASO (MD +1.25 m) and SNOTEL (+0.71 m to +1.55 m) snow depths. Overall, using ASO as an additional snow depth reference data set at discrete point locations in the model domain showed no consistent over or under-simulation for iSnobal. After the seasonal snow depth peak was reached, simulated snow depths around all three SNOTEL stations deviated from observations and the range of simulated values increased. Notably, the date for snow disappearance was consistently simulated later relative to observations across all years but varied in magnitude. For instance, the difference between iSnobal and all SNOTEL

255   sites was between 11 to 59 days in 2018 and -8 to 59 days in 2019. An overview of the differences between observations and simulations is shown in Table 1. Disagreement in snowmelt rates and snow disappearance is attributed primarily to errors in net solar radiation, which is discussed further in Section 6.4. Overall, the snow depth comparison to observations over multiple years showed that the model can capture peak snow depth timing and magnitude.
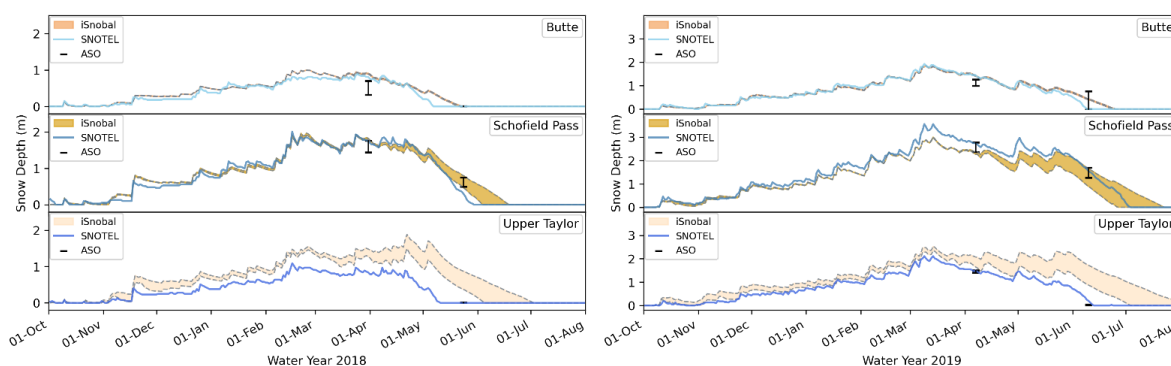
Figure 4 – Snow Depth comparison between iSnobal and SNOTEL sites for the years 2018 (left) and 2019 (right). The orange shaded areas represent the range of 2x2 grid cell values from iSnobal surrounding the site. The ranges of the grid cell values from ASO surveys are shown by the black bars. Note the difference y-scales between 2018 and 2019.

Table 1 – Overview of date differences for last day with snow present between iSnobal and SNOTEL sites.

SNOTEL site	**Melt dates**	**2018**	**2019**	**2020**	**2021**
Butte	*SNOTEL*	05/06	06/08	05/12	05/12
	iSnobal	05/24 to 05/25	06/24 to 06/26	05/26 to 05/28	05/31 to 06/02
	Difference	18 – 19 days	16 – 18 days	14 – 16 days	19 – 21 days
Schofield Pass	*SNOTEL*	05/29	07/03	06/03	06/02
	iSnobal	06/09 to 06/23	06/25 to 07/25	05/29 to 06/17	06/05 to 06/20
	Difference	11 – 25 days	-8 – 22 days	-5 – 14 days	3 – 18 days
Upper Taylor	*SNOTEL*	05/10	06/12	05/13	05/13
	iSnobal	06/10 to 07/08	07/03 to 08/10	05/31 to 07/05	06/06 to 07/05
	Difference	31 – 59 days	21 – 59 days	18 – 53 days	24 – 53 days

5.3 ASO comparison

260   Integrated over the full basin, simulated snow depths agreed with ASO lidar snow depths, with a grid cell median difference of
0.02 m (early survey) and 0.00 m (late survey) in 2018, 0.20 m and 0.00 m in 2019, and 0.14 m in 2020. Generally, between two
flights in the same season, the agreement was best during late flights in the middle and lower HRU (Figure 5a and 5b). An aerial
overview for all flights can be found in Supplement Figures S3, S4, and S5 to this paper showing the difference per 50 m grid cell.
Within low, mid, and high elevations HRUs, the widest range in the Δ snow depth distribution was consistently found at the higher
265   elevations (Standard Deviation 0.5 m in 2018; 0.9 m to 1.0 m in 2019), while the narrowest range was found at the lower elevations
HRU (Standard Deviation 0.0 m to 0.2 m in 2018; 0.1 m to 0.6 m in 2019). The middle elevations HRU was somewhere in between
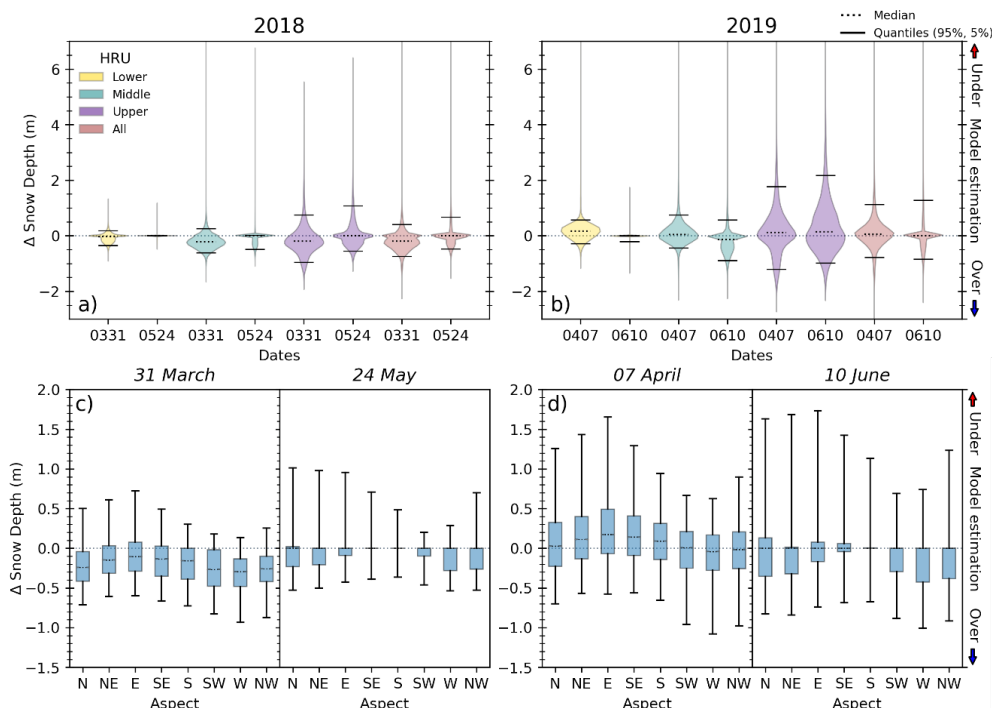
Figure 5 – Snow Depth Differences for early and late surveys for the years 2018 and 2019 between ASO and iSnobal. Figure a) and b) categorize the differences by elevation HRU (low, middle, upper) with the 'All' showing the basin-wide difference. Figure c) and d) bin the difference by aspect. Note the different y-scales between top and bottom figures.

(Standard Deviation 0.2 to 0.3 m in 2018; 0.5 m in 2019). The distributions of Δ snow depth for the late survey in each year showed positive biases, indicating a general overestimation of snow depths by iSnobal, consistent with the observed slower snow depth decrease during the snowmelt season at the SNOTEL sites (Figure 4).

270 The snow depth differences binned by aspect for the entire watershed indicated a bias, with variation during flight dates and the two years (Figure 5c and 5d). In both early flights, higher snow depth was measured on eastern aspects relative to other aspects, and the widest ranges in snow depth differences were on northern aspects in both late flights. The closest agreement between modeled and ASO lidar snow depths was on south-facing slopes during late flights.

5.4 Stream Gauge comparison

275 The watershed 7-day moving average of simulated iSnobal SWI followed the hydrograph timing and magnitude pattern measured at the stream gauge (Figure 6). During the annual snow melt pulse, the iSnobal SWI stayed higher relative to the measured surface water at the gauge. The time-series magnitude difference between measured discharge and simulated SWI was highest in 2018, the lowest snow year, and closest in 2019, the highest snow year. Although similar in the last days with snow depth across the SNOTEL sites in 2020 and 2021 (Table 1), the simulated SWI was different between the two years and the hydrograph had a

280 higher peak in 2020, with a lower in 2021, following the measured stream gauge values. The later than observed simulated iSnobal snow disappearance dates were also apparent in this comparison; a longer time lag would be expected during the receding limb of the hydrograph because the SWI is not instantaneously at the gauge. Still, the general patterns and magnitude are promising in that there is no under-forecasted SWI at any point in the melt season.

5.5 SNOW-17 comparison

285 Generally, precipitation used as an input to SNOW-17 was consistently higher than the HRRR precipitation input used for iSnobal across all years. The difference ranged from HRRR being 25% (2021) to 5% (2018) lower, integrated across all HRUs. A summary of the comparison, per HRU and for the full watershed, is in Table 2. Using SNOW-17 as the reference, the daily total amount difference was consistent across the HRUs and years with no high ratio differences (Supplement Figure S7). For total amounts per HRU, the poorest agreement was in the lower HRU in 2020, with HRRR 36% lower. The best agreement was found in the middle

290 HRU in 2018, with a match of 99%. The differences per HRU were not correlated to whether it was a high or low snow year, with similar agreement in 2018 (lowest snow) and 2019 (highest snow). The poorest overall agreement (2020 and 2021) had higher precipitation amount for SNOW-17 (2020: 18%, 2021; 25%), which was not reflected in the SNOTEL site comparison. The snow depth across all sites 2020 had a mean difference between of -0.20 m and +0.23 m and 2021 a mean difference of +0.02 m and -
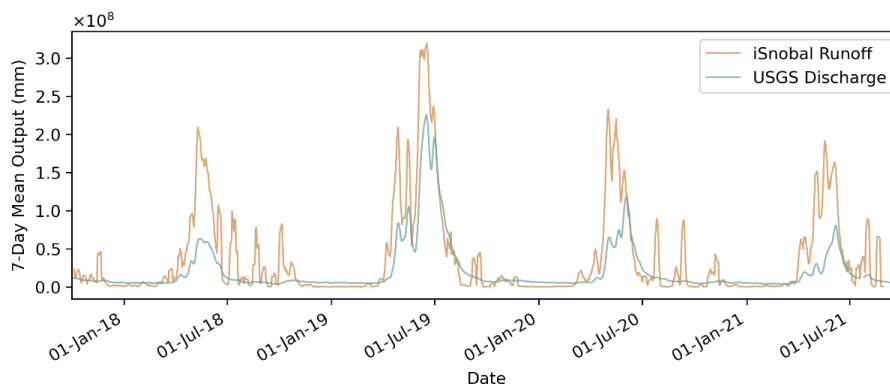
Figure 6 – Time series comparison of simulated iSnobal SWI against the measured USGS stream gauge discharge across the four water years.

Table 2 – Overview of precipitation inputs and SWE outputs for iSnobal and SNOW-17 classified by HRU.

HRU		**2018**		**2019**		**2020**		**2021**	
		Precip.	*SWE*	*Precip.*	*SWE*	*Precip.*	*SWE*	*Precip.*	*SWE*
Lower	*iSnobal*	300	7352	496	24976	265	12897	325	12183
	Snow-17	333	5888	566	26653	413	16816	418	13509
	Ratio	90%	125%	88%	94%	64%	77%	78%	90%
Middle	*iSnobal*	491	30567	796	66744	471	34448	468	31574
	Snow-17	495	25375	859	67347	573	39788	606	37270
	Ratio	99%	120%	93%	99%	82%	87%	77%	85%
Upper	*iSnobal*	667	45639	1076	107478	658	52176	599	49037
	Snow-17	707	59676	1196	135108	723	75563	832	74739
	Ratio	94%	76%	90%	80%	91%	69%	72%	66%
All	*iSnobal*	1458	83558	2368	199198	1394	99521	1392	92794
	Snow-17	1535	90939	2621	229108	1709	132167	1856	125518
	Total	95%	92%	90%	87%	82%	75%	75%	74%

Note: Precipitation (Precip.) and SWE values are shown in mm.
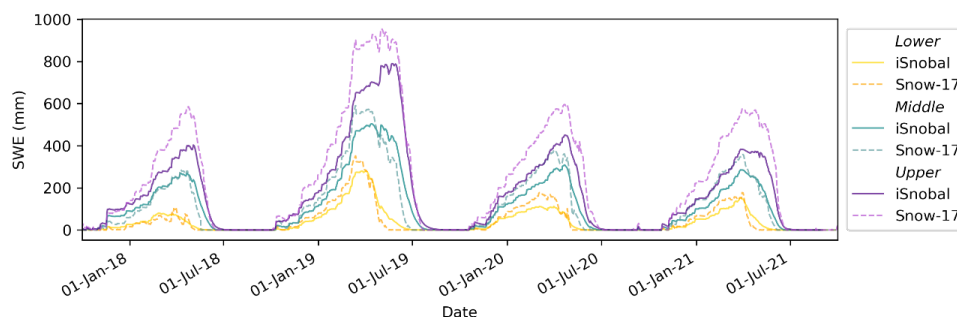
Figure 7 – Total SWE per HRU showed higher amounts in SNOW-17 than iSnobal. The lower HRU agreed best, while the upper had more peak SWE in SNOW-17. The temporal pattern for SWE agreed between the two models, having slightly longer presence of snow in iSnobal.

0.17 m in the pre-melt season (Supplement Figure S2). Both of the years had similar HRRR total precipitation amounts compared

295   to 2018 (Differences 2020: -64 mm, 2021: -66 mm), which is also supported by the similar depth at all SNOTEL sites as 2018 (Supplemental Figure S1).

Across the four years, all three HRUs showed similar temporal patterns for daily total SWE in the snowpack although iSnobal SWE was lower in magnitude (Figure 7) and expected following the precipitation comparison (Table 2). Consequently, he largest difference between the two models was in the upper HRU (iSnobal between 34% to 20% lower), with less difference in the middle

300   (iSnobal between 20% higher and 15% lower) and lower (iSnobal between 25% higher and 23% lower) HRUs. As with the SNOTEL depth comparison, the basin SWE from iSnobal showed longer persistence of snow compared to SNOW-17. This lag is most apparent in the lower and middle HRU, with the upper HRU having similar snow depletion timing.

6. Discussion

6.1 HRRR Precipitation

305 The results for the snow depths comparison to SNOTEL and ASO indicated that the HRRR precipitation allowed iSnobal to simulate the snow mass balance well. This is promising because HRRR data are distributed at 3 km resolution and are much coarser than the 50 m model output resolution, which is needed to resolve the different physical processes influencing the snowpack evolution in this type of terrain (Winstral et al., 2014). The difference in resolutions makes it challenging to properly adjust for the topographic precipitation differences, especially with the model domain's high vertical relief (1420 m). Kilometer scale NWP

310 model resolutions are known to underestimate snowfall at higher elevations, and complex terrain is particularly challenging to simulate snowpack evolution with inconsistent snowfall trends (Ikeda 2010). The current solutions to 'bias correct' and improve NWP precipitation based on topography are basin and application specific. For example, Bellaire et al. (2011, 2013) applied a constant correction factor and Griessinger et al. (2019) corrected and filtered with observations from a dense in-situ network. These approaches require in-situ observation and basin-specific knowledge that is not always available, reducing transferability to other

315 regions. Ultimately, the fewer corrections needed to forcing inputs results in greater potential to scale and adapt model setups into forecast operations. The presented workflow here had no changes to the HRRR inputs and precipitation was used 'as is'.

Given the different methods to determine precipitation in HRRR and as inputs to SNOW-17, a match between the two was not expected. The calibration process for SNOW-17 precipitation inputs uses spatially sparse in-situ point measurements and empirical data from previous water years. As an atmospheric model, HRRR is a product of assimilated observation, physically based

320 modeling, and a fundamentally different approach. Neither set of precipitation values were considered the truth, and accurately measuring precipitation is an unsolved challenge in mountain terrain. Additional work is needed to understand the variation in HRRR values relative to the calibrated precipitation used by the CBRFC across these water years (i.e poorer agreement in 2020 and 2021).

6.2 Comparison Data Sources

325 The snow depth comparison of this work used in-situ point observations and aerial spatial measurements. Both sources had no consistent agreement, with the spatial measurements tending to be lower than the point data. This underestimation has been shown to exist when comparing point data to spatial averages of snow depth from lidar (Trujillo and Lehning, 2015). Similarly, in-situ snow depth estimates from point observation stations, such as SNOTEL, are known to only represent a small surrounding footprint because of the large heterogeneity of snow depth in alpine environments (Molotch and Bales, 2005). This limitation, in part, can

330 explain the higher spread of the iSnobal snow depths to the SNOTEL stations, as the values represent a larger area around them (Figure 3). The strength of SNOTEL station data is as long-term historical records, from which index methods could be developed and help understand changes over long timeframes (Harpold et al., 2012; Musselman et al., 2021; Trujillo and Molotch, 2014). In the case of this work, it was the only source available to allow a model performance assessment over multiple years. The results from the SNOTEL comparison gave confidence that the HRRR forcing inputs provided a quality long-term input source, in terms

335 of capturing peak snow depth, for a watershed with only sparse in-situ meteorological observations across different snow seasons. The addition of aerial observations, such as ASO, has improved the ability to retrieve snow depth over large areas and supplies valuable validation data used in many studies (Brandt et al., 2020; Hedrick et al., 2018; McGrath et al., 2019). In this work, the ASO maps enabled a spatial comparison that was impossible in the past. The comparison identified differences in snow depth at high elevations and across aspects that are not possible with SNOTEL stations, which are generally located in relatively flat middle

340 and lower elevations (e.g., below 3261 m in ERW). Additionally, the snow depth disagreements between measured ASO and

SNOTEL highlighted that SNOTEL observations could not represent snow conditions at 50 m model output resolutions either, and caution is urged when using SNOTEL snow depth data as 'truth' for spatially distributed models. Likewise, the inconsistent comparison results to SNOTEL showed that coarser aerial product resolutions should also not be treated as truth, and snow depths can vary within short distances due to the high spatial variability of mountain terrain.

345 **6.3 Physically Based Models**

Existing studies using long-term records of SNOTEL measurements have identified a need for physically based modeling approaches (Harpold et al., 2012; Musselman et al., 2021; Trujillo and Molotch, 2014) as they better show the impact of the current and improve the projection of the future changes to the water supply. Physically based models are capable of accounting for scenarios such as shifting snowmelt rates (Musselman et al., 2017), changes to the length of snow accumulation and melt season

350 (Trujillo and Molotch, 2014), and accelerated melt due to darker snow (Skiles et al., 2018), through the calculation of energy terms such as net solar radiation, a main driver of snowmelt (Marks and Dozier, 1992). Physically based models also do not have to rely on region-specific calibrated parameters or forecaster experience when adapting to conditions outside the long-term calibration data. This ability, in part, is due to including more meteorological observations, removing the dependence on historical calibration records.

355 Gradually adding physically based models into operational environments, with architectures presented in this work, has value because they can provide information about the response of the snowpack to current environmental perturbations, which may improve the confidence of the water supply forecast. Current models, such as SNOW-17, are tested and proven in operations, and a drop-in replacement is impractical. However, physically based models have the technical capability and scalability to run in parallel and supplement the established methods. Their addition into operational environments will enhance the quality and expand

360 the ability to adapt to current and future water supply forecast needs.

6.4 Improvements to iSnobal

The consistent longer presence of snow in iSnobal-HRRR relative to the observations across the simulated years highlighted an area for improvement. One cause for the delay is attributed to the too low amount of calculated solar radiation by SMRF, not providing enough energy to drive snowmelt in iSnobal. An obvious option that influences the calculation is the snow albedo time-

365 decay function, which has caused high uncertainty in many different model types and scales (Chen et al., 2014; Clark et al., 2015; Krinner et al., 2018; Qu and Hall, 2014; Ryken et al., 2020). The decay function determines the snow albedo based on the time of the last snowfall when the albedo gets reset, and the decay starts anew. A drawback of this approach is excluding other events that change the albedo, such as dust deposition. Solutions for the 1-d Snobal model improved the simulated snowmelt timing and forced the model with observed snow albedo (Miller et al., 2016; Skiles and Painter, 2019; Skiles et al., 2015, 2012). Scaling this solution

370 and adapting it into spatially distributed models requires data sources with daily updated and spatially complete snow albedo, which are available today from remote sensing observations. For instance, the combined MODIS Snow Covered Area and Grain Size (MODSCAG) and Dust Radiative Forcing (MODDRFS) in Snow (Rittger et al., 2020) provides daily observation with 500 m spatial resolution. This spatial and temporal resolution fulfills the requirements of a model data source. With the demonstrated need for improved snow disappearance dates of this work, improved results by using observations in other work, and the availability

375 of remote sensing products, we suggest integrating remotely sensed snow albedo into iSnobal.

Though relatively sparse in time, the spatial snow depth comparison results highlighted another area to target with iSnobal-HRRR. The snow depths differences by aspect (Figures 5c and 5d) indicated an iSnobal energy balance issue as there was no strong aspect bias coming from the HRRR precipitation data (Supplement Figure S6). The closer agreements on the south-facing aspect suggest

that improving the incoming solar radiation could help address this model bias. Solar radiation is currently a topographically

380 adjusted calculation (Dozier 1990) by SMRF. One alternative to this approach is to use the supplied values by HRRR, reducing model complexity and computation times. The addition of remotely sensed albedo and alternative handling for incoming solar radiation will be the follow-up effort for iSnobal to this work.

7 Conclusions

This work presented and evaluated the spatially distributed iSnobal model forced with HRRR meteorological data to expand the

385 model options and to support operational water forecasts for the CBRFC. The model was assessed over one representative headwater basin in the CRB with an area of 1373 km² for four consecutive water years (2018 - 2021) at a 50 m spatial resolution and hourly time steps. There were several key outcomes from this effort: (1) Execution times from one to the next day and total storage requirements would allow operational forecasters to run iSnobal-HRRR alongside current production environments (2) HRRR provided meteorological input data that enabled iSnobal to simulate close to the observed snow depths up to peak

390 accumulation (3) iSnobal radiation calculations need revisions to improve melt timing and to address geographic aspect bias (4) Simulated timing and magnitude of iSnobal SWI followed the observed hydrograph at the basin stream gauge.

From the model comparison, the iSnobal SWE was lower than the SNOW-17 SWE and consistent with the lower precipitation inputs from HRRR than the SNOW-17 inputs. iSnobal had lower snow depths at higher elevations relative to aerial observations and was attributed to the coarser model output resolution of HRRR relative to the topography and the simulated spatial resolution.

395 Model runs in additional basins are ongoing and will allow further evaluation if this is consistent. Despite these differences, iSnobal simulated snow depths close to measured values across the watershed up to the melt period. Once snowmelt set in, iSnobal snow depths showed greater disagreement than the observed in-situ measurement sites and simulated longer snow persistence. The discrepancy between observed and simulated snowmelt timing, and therefore magnitude, was consistent across the years, including above-average and below-average snow years. Accurately simulating snow depletion timing is important for operational adoption.

400 Future work to address snowmelt timing aims to improve snow energy balance calculations, specifically by using remotely observed snow albedo data and updating the net solar radiation treatment in iSnobal. Nevertheless, as the world transitions into a future that is less similar to the past and statistical models become less reliable, this work showed that iSnobal-HRRR could be a valuable supplement to operational water supply forecasting methods in snow-dominated regions.

Code availability

405 The software components used to run the model and analyze the results are publicly available. iSnobal model components are available via the USDA ARS NWRC GitHub page: https://github.com/USDA-ARS-NWRC. For this study, GitHub forks for SMRF (https://doi.org/10.5281/zenodo.6543935), AWSM (https://doi.org/10.5281/zenodo.6543919), and weather forecast retrieval (https://doi.org/10.5281/zenodo.6543579) were created to capture the model code at the time of completing this study as no official version was released. The forks can be found under https://github.com/UofU-Cryosphere. Additions to model setup and

410 result analysis code are stored on https://github.com/UofU-Cryosphere/isnoda (https://doi.org/10.5281/zenodo.6543995).

Data availability

The following datasets were used for the model runs and comparisons:

- LANDFIRE Program: Data Product Mosaic Downloads: https://landfire.gov/version_download.php, last access: 28 February 2022.
415 - NOAA The High-Resolution Rapid Refresh (HRRR): https://rapidrefresh.noaa.gov/hrrr/, last access: 28 February 2022.
- NRCS National Water and Climate Center | SNOTEL | SWE Data: https://www.wcc.nrcs.usda.gov/snow/SNOTEL-wedata.html, last access: 28 February 2022.
- The National Map | U.S. Geological Survey: https://www.usgs.gov/programs/national-geospatial-program/national-map, last access: 28 February 2022.
420 - USGS Surface Water data for USA: USGS Surface-Water Daily Statistics: https://waterdata.usgs.gov/nwis/dvstat/?site_no=09112500&referred_module=sw&format=sites_selection_links, last access: 28 February 2022.
- Painter, T. H.: ASO L4 Lidar Snow Depth 50m UTM Grid, Version 1. [USCOGE]. Boulder, Colorado USA. NASA National Snow and Ice Data Center Distributed Active Archive Center, NSIDC, https://doi.org/10.5067/STOT5I0U1WVI, 2018.

425 **Author contributions**

JM and MS conceptualized the overall study, with helpful contributions from all authors. JM performed the model runs and analysis. PK provided CBRFC data and support. MS provided financial support for the study. JM wrote the first draft of the manuscript, which was then contributed to by all authors.

Acknowledgement

430 The support and resources from the Center for High Performance Computing (CHPC) at the University of Utah are gratefully acknowledged.
The USDA is an equal opportunity provider and employer.

Competing interests

The authors declare that they have no conflict of interest.

435 **Financial support**

This work was funded by the NASA ESD Applied Sciences - Water Resources (grant number 80NSSC19K1243)

References

Anderson, E. A.: A point energy and mass balance model of a snow cover, 1976.
Automated Water Supply Model — awsm documentation: https://awsm.readthedocs.io/en/latest/readme.html, last access: 28
440 February 2022.
Spatial Modeling for Resources Framework — SMRF documentation: https://smrf.readthedocs.io/en/latest/, last access: 28 February 2022.

Ayers, J., Ficklin, D. L., Stewart, I. T., and Strunk, M.: Comparison of CMIP3 and CMIP5 projected hydrologic conditions over the Upper Colorado River Basin, 36, 3807–3818, https://doi.org/10.1002/joc.4594, 2016.

445 Bellaire, S., Jamieson, J. B., and Fierz, C.: Forcing the snow-cover model SNOWPACK with forecasted weather data, 5, 1115–1125, https://doi.org/10.5194/tc-5-1115-2011, 2011.

Bellaire, S., Jamieson, J. B., and Fierz, C.: Corrigendum to "Forcing the snow-cover model SNOWPACK with forecasted weather data" published in The Cryosphere, 5, 1115–1125, 2011, 7, 511–513, https://doi.org/10.5194/tc-7-511-2013, 2013.

Benjamin, S. G., Weygandt, S. S., Brown, J. M., Hu, M., Alexander, C. R., Smirnova, T. G., Olson, J. B., James, E. P., Dowell, D.
450 C., Grell, G. A., Lin, H., Peckham, S. E., Smith, T. L., Moninger, W. R., Kenyon, J. S., and Manikin, G. S.: A North American Hourly Assimilation and Model Forecast Cycle: The Rapid Refresh, 144, 1669–1694, https://doi.org/10.1175/MWR-D-15-0242.1, 2016.

Brandt, W. T., Bormann, K. J., Cannon, F., Deems, J. S., Painter, T. H., Steinhoff, D. F., and Dozier, J.: Quantifying the Spatial Variability of a Snowstorm Using Differential Airborne Lidar, Water Resour. Res., 56, https://doi.org/10.1029/2019WR025331,
455 2020.

Brun, E., Martin, E., Simon, V., Gendre, C., and Coleou, C.: An Energy and Mass Model of Snow Cover Suitable for Operational Avalanche Forecasting, 35, 333–342, https://doi.org/10.3189/S0022143000009254, 1989.

Bryant, A. C., Painter, T. H., Deems, J. S., and Bender, S. M.: Impact of dust radiative forcing in snow on accuracy of operational runoff prediction in the Upper Colorado River Basin: DUST IN SNOW IMPACT ON STREAMFLOW, Geophys. Res. Lett., 40,
460 3945–3949, https://doi.org/10.1002/grl.50773, 2013.

Byteway, J. L., Kummerow, C. D., and Alexander, C.: A Features-Based Assessment of the Evolution of Warm Season Precipitation Forecasts from the HRRR Model over Three Years of Development, 32, 1841–1856, https://doi.org/10.1175/WAF-D-17-0050.1, 2017.

Chen, F., Barlage, M., Tewari, M., Rasmussen, R., Jin, J., Lettenmaier, D., Livneh, B., Lin, C., Miguez-Macho, G., Niu, G.-Y.,
465 Wen, L., and Yang, Z.-L.: Modeling seasonal snowpack evolution in the complex terrain and forested Colorado Headwaters region: A model intercomparison study, J. Geophys. Res. Atmos., 119, 13,795-13,819, https://doi.org/10.1002/2014JD022167, 2014.

Cho, E., McCrary, R. R., and Jacobs, J. M.: Future Changes in Snowpack, Snowmelt, and Runoff Potential Extremes Over North America, 48, e2021GL094985, https://doi.org/10.1029/2021GL094985, 2021.

Christensen, N. S. and Lettenmaier, D. P.: A multimodel ensemble approach to assessment of climate change impacts on the
470 hydrology and water resources of the Colorado River Basin, 11, 1417–1434, https://doi.org/10.5194/hess-11-1417-2007, 2007.

Clark, M. P., Nijssen, B., Lundquist, J. D., Kavetski, D., Rupp, D. E., Woods, R. A., Freer, J. E., Gutmann, E. D., Wood, A. W., Gochis, D. J., Rasmussen, R. M., Tarboton, D. G., Mahat, V., Flerchinger, G. N., and Marks, D. G.: A unified approach for process-based hydrologic modeling: 2. Model implementation and case studies, 51, 2515–2542, https://doi.org/10.1002/2015WR017200, 2015.

475 Council, N. R.: Toward a new advanced hydrologic prediction service (AHPS), The National Academies Press, Washington, DC, 84 pp., https://doi.org/10.17226/11598, 2006.

Dettinger, M., Udall, B., and Georgakakos, A.: Western water and climate change, 25, 2069–2093, https://doi.org/10.1890/15-0938.1, 2015.

Dozier, J. and Frew, J.: Rapid calculation of terrain parameters for radiation modeling from digital elevation data, 28, 963–969,
480 https://doi.org/10.1109/36.58986, 1990.

Essery, R.: A factorial snowpack model (FSM 1.0), Geosci. Model Dev., 8, 3867–3876, https://doi.org/10.5194/gmd-8-3867-2015, 2015.

Feng, S. and Hu, Q.: Changes in winter snowfall/precipitation ratio in the contiguous United States, 112, https://doi.org/10.1029/2007JD008397, 2007.

485   Forthofer, J. M., Butler, B. W., Wagenbrenner, N. S., Forthofer, J. M., Butler, B. W., and Wagenbrenner, N. S.: A comparison of three approaches for simulating fine-scale surface winds in support of wildland fire management. Part I. Model formulation and comparison against measurements, Int. J. Wildland Fire, 23, 969–981, https://doi.org/10.1071/WF12089, 2014.

Franz, K. J., Hogue, T. S., and Sorooshian, S.: Operational snow modeling: Addressing the challenges of an energy balance model for National Weather Service forecasts, Journal of Hydrology, 360, 48–66, https://doi.org/10.1016/j.jhydrol.2008.07.013, 2008.

490   Franz, K. J., Butcher, P., and Ajami, N. K.: Addressing snow model uncertainty for hydrologic prediction, Advances in Water Resources, 33, 820–832, https://doi.org/10.1016/j.advwatres.2010.05.004, 2010.

Garen, D. C. and Marks, D.: Spatially distributed energy balance snowmelt modelling in a mountainous river basin: estimation of meteorological inputs and verification of model results, Journal of Hydrology, 315, 126–153, https://doi.org/10.1016/j.jhydrol.2005.03.026, 2005.

495   Gowan, T. A., Horel, J. D., Jacques, A. A., and Kovac, A.: Using Cloud Computing to Analyze Model Output Archived in Zarr Format, 1, https://doi.org/10.1175/JTECH-D-21-0106.1, 2022.

Griessinger, N., Schirmer, M., Helbig, N., Winstral, A., Michel, A., and Jonas, T.: Implications of observation-enhanced energy-balance snowmelt simulations for runoff modeling of Alpine catchments, Advances in Water Resources, 133, 103410, https://doi.org/10.1016/j.advwatres.2019.103410, 2019.

500   Harpold, A., Brooks, P., Rajagopal, S., Heidbuchel, I., Jardine, A., and Stielstra, C.: Changes in snowpack accumulation and ablation in the intermountain west, 48, https://doi.org/10.1029/2012WR011949, 2012.

Havens, S., Marks, D., Kormos, P., and Hedrick, A.: Spatial Modeling for Resources Framework (SMRF): A modular framework for developing spatial forcing data for snow modeling in mountain basins, Computers & Geosciences, 109, 295–304, https://doi.org/10.1016/j.cageo.2017.08.016, 2017.

505   Havens, S., Marks, D., FitzGerald, K., Masarik, M., Flores, A. N., Kormos, P., and Hedrick, A.: Approximating Input Data to a Snowmelt Model Using Weather Research and Forecasting Model Outputs in Lieu of Meteorological Measurements, 20, 847–862, https://doi.org/10.1175/JHM-D-18-0146.1, 2019.

Havens, S., Marks, D., Sandusky, M., Hedrick, A., Johnson, M., Robertson, M., and Trujillo, E.: Automated Water Supply Model (AWSM): Streamlining and standardizing application of a physically based snow model for water resources and reproducible

510   science, Computers & Geosciences, 144, 104571, https://doi.org/10.1016/j.cageo.2020.104571, 2020.

He, M., Hogue, T. S., Franz, K. J., Margulis, S. A., and Vrugt, J. A.: Characterizing parameter sensitivity and uncertainty for a snow model across hydroclimatic regimes, Advances in Water Resources, 34, 114–127, https://doi.org/10.1016/j.advwatres.2010.10.002, 2011.

Hedrick, A. R., Marks, D., Havens, S., Robertson, M., Johnson, M., Sandusky, M., Marshall, H., Kormos, P. R., Bormann, K. J.,

515   and Painter, T. H.: Direct Insertion of NASA Airborne Snow Observatory-Derived Snow Depth Time Series Into the iSnobal Energy Balance Snow Model, Water Resour. Res., 54, 8045–8063, https://doi.org/10.1029/2018WR023190, 2018.

Hedrick, A. R., Marks, D., Marshall, H., McNamara, J., Havens, S., Trujillo, E., Sandusky, M., Robertson, M., Johnson, M., Bormann, K. J., and Painter, T. H.: From Drought to Flood: A Water Balance Analysis of the Tuolumne River Basin during Extreme Conditions (2015 – 2017), Hydrological Processes, hyp.13749, https://doi.org/10.1002/hyp.13749, 2020.

520   Ikeda, K., Rasmussen, R., Liu, C., Newman, A., Chen, F., Barlage, M., Gutmann, E., Dudhia, J., Dai, A., Luce, C., and Musselman, K.: Snowfall and snowpack in the Western U.S. as captured by convection permitting climate simulations: current climate and pseudo global warming future climate, Clim Dyn, 57, 2191–2215, https://doi.org/10.1007/s00382-021-05805-w, 2021.

Iwamoto, K., Yamaguchi, S., Nakai, S., and Sato, A.: Forecasting Experiments Using the Regional Meteorological Model and the Numerical Snow Cover Model in the Snow Disaster Forecasting System, 30, 35–43, https://doi.org/10.2328/jnds.30.35, 2008.

525 Knowles, N., Dettinger, M. D., and Cayan, D. R.: Trends in Snowfall versus Rainfall in the Western United States, 19, 4545–4559, https://doi.org/10.1175/JCLI3850.1, 2006.

Kormos, P. R., Marks, D., McNamara, J. P., Marshall, H. P., Winstral, A., and Flores, A. N.: Snow distribution, melt and surface water inputs to the soil in the mountain rain–snow transition zone, Journal of Hydrology, 519, 190–204, https://doi.org/10.1016/j.jhydrol.2014.06.051, 2014.

530 Krinner, G., Derksen, C., Essery, R., Flanner, M., Hagemann, S., Clark, M., Hall, A., Rott, H., Brutel-Vuilmet, C., Kim, H., Ménard, C. B., Mudryk, L., Thackeray, C., Wang, L., Arduini, G., Balsamo, G., Bartlett, P., Boike, J., Boone, A., Chéruy, F., Colin, J., Cuntz, M., Dai, Y., Decharme, B., Derry, J., Ducharne, A., Dutra, E., Fang, X., Fierz, C., Ghattas, J., Gusev, Y., Haverd, V., Kontu, A., Lafaysse, M., Law, R., Lawrence, D., Li, W., Marke, T., Marks, D., Ménégoz, M., Nasonova, O., Nitta, T., Niwano, M., Pomeroy, J., Raleigh, M. S., Schaedler, G., Semenov, V., Smirnova, T. G., Stacke, T., Strasser, U., Svenson, S., Turkov, D.,

535 Wang, T., Wever, N., Yuan, H., Zhou, W., and Zhu, D.: ESM-SnowMIP: assessing snow models and quantifying snow-related climate feedbacks, 11, 5027–5049, https://doi.org/10.5194/gmd-11-5027-2018, 2018.

Lehning, M., Bartelt, P., Brown, B., Fierz, C., and Satyawali, P.: A physical SNOWPACK model for the Swiss avalanche warning: Part II. Snow microstructure, Cold Regions Science and Technology, 35, 147–167, https://doi.org/10.1016/S0165-232X(02)00073-3, 2002.

540 Li, D., Wrzesien, M. L., Durand, M., Adam, J., and Lettenmaier, D. P.: How much runoff originates as snow in the western United States, and how will that change in the future?, Geophys. Res. Lett., 44, 6163–6172, https://doi.org/10.1002/2017GL073551, 2017.

Link, T. E., Marks, D., and Hardy, J. P.: A deterministic method to characterize canopy radiative transfer properties, 18, 3583–3594, https://doi.org/10.1002/hyp.5793, 2004.

Liston, G. E. and Elder, K.: A Distributed Snow-Evolution Modeling System (SnowModel), 7, 1259–1276,

545 https://doi.org/10.1175/JHM548.1, 2006.

Marks, D. and Dozier, J.: Climate and energy exchange at the snow surface in the Alpine Region of the Sierra Nevada: 2. Snow cover energy balance, 28, 3043–3054, https://doi.org/10.1029/92WR01483, 1992.

Marks, D., Dozier, J., and Davis, R. E.: Climate and energy exchange at the snow surface in the Alpine Region of the Sierra Nevada: 1. Meteorological measurements and monitoring, 28, 3029–3042, https://doi.org/10.1029/92WR01482, 1992.

550 Marks, D., Domingo, J., Susong, D., Link, T., and Garen, D.: A spatially distributed energy balance snowmelt model for application in mountain basins, 13, 26, 1999.

McGrath, D., Webb, R., Shean, D., Bonnell, R., Marshall, H.-P., Painter, T. H., Molotch, N. P., Elder, K., Hiemstra, C., and Brucker, L.: Spatially Extensive Ground-Penetrating Radar Snow Depth Observations During NASA's 2017 SnowEx Campaign: Comparison With In Situ, Airborne, and Satellite Observations, Water Resour. Res., 55, 10026–10036,

555 https://doi.org/10.1029/2019WR024907, 2019.

Miller, S. D., Wang, F., Burgess, A. B., Skiles, S. M., Rogers, M., and Painter, T. H.: Satellite-Based Estimation of Temporally Resolved Dust Radiative Forcing in Snow Cover, 17, 1999–2011, https://doi.org/10.1175/JHM-D-15-0150.1, 2016.

Molotch, N. P. and Bales, R. C.: Scaling snow observations from the point to the grid element: Implications for observation network design, Water Resour. Res., 41, https://doi.org/10.1029/2005WR004229, 2005.

560 Mote, P. W., Li, S., Lettenmaier, D. P., Xiao, M., and Engel, R.: Dramatic declines in snowpack in the western US, 1, 2, https://doi.org/10.1038/s41612-018-0012-1, 2018.

Musselman, K. N., Clark, M. P., Liu, C., Ikeda, K., and Rasmussen, R.: Slower snowmelt in a warmer world, Nature Clim Change, 7, 214–219, https://doi.org/10.1038/nclimate3225, 2017.

Musselman, K. N., Addor, N., Vano, J. A., and Molotch, N. P.: Winter melt trends portend widespread declines in snow water
565   resources, Nat. Clim. Chang., 11, 418–424, https://doi.org/10.1038/s41558-021-01014-9, 2021.

Painter, T. H., Berisford, D. F., Boardman, J. W., Bormann, K. J., Deems, J. S., Gehrke, F., Hedrick, A., Joyce, M., Laidlaw, R., Marks, D., Mattmann, C., McGurk, B., Ramirez, P., Richardson, M., Skiles, S. M., Seidel, F. C., and Winstral, A.: The Airborne Snow Observatory: Fusion of scanning lidar, imaging spectrometer, and physically-based modeling for mapping snow water equivalent and snow albedo, Remote Sensing of Environment, 184, 139–152, https://doi.org/10.1016/j.rse.2016.06.018, 2016.

570 Painter, T. H., Skiles, S. M., Deems, J. S., Brandt, W. T., and Dozier, J.: Variation in Rising Limb of Colorado River Snowmelt Runoff Hydrograph Controlled by Dust Radiative Forcing in Snow, https://doi.org/10.1002/2017GL075826, 2018.

Qu, X. and Hall, A.: On the persistent spread in snow-albedo feedback, Clim Dyn, 42, 69–81, https://doi.org/10.1007/s00382-013-1774-0, 2014.

Rittger, K., Raleigh, M. S., Dozier, J., Hill, A. F., Lutz, J. A., and Painter, T. H.: Canopy Adjustment and Improved Cloud Detection
575   for Remotely Sensed Snow Cover Mapping, 56, e2019WR024914, https://doi.org/10.1029/2019WR024914, 2020.

Ryken, A., Bearup, L. A., Jefferson, J. L., Constantine, P., and Maxwell, R. M.: Sensitivity and model reduction of simulated snow processes: Contrasting observational and parameter uncertainty to improve prediction, Advances in Water Resources, 135, 103473, https://doi.org/10.1016/j.advwatres.2019.103473, 2020.

Schirmer, M. and Jamieson, B.: Verification of analysed and forecasted winter precipitation in complex terrain, 9, 587–601,
580   https://doi.org/10.5194/tc-9-587-2015, 2015.

Schmucki, E., Marty, C., Fierz, C., and Lehning, M.: Evaluation of modelled snow depth and snow water equivalent at three contrasting sites in Switzerland using SNOWPACK simulations driven by different meteorological data input, Cold Regions Science and Technology, 99, 27–37, https://doi.org/10.1016/j.coldregions.2013.12.004, 2014.

Skiles, S. M. and Painter, T.: Daily evolution in dust and black carbon content, snow grain size, and snow albedo during snowmelt,
585   Rocky Mountains, Colorado, 63, 118–132, https://doi.org/10.1017/jog.2016.125, 2017.

Skiles, S. M. and Painter, T. H.: Toward Understanding Direct Absorption and Grain Size Feedbacks by Dust Radiative Forcing in Snow With Coupled Snow Physical and Radiative Transfer Modeling, Water Resour. Res., 55, 7362–7378, https://doi.org/10.1029/2018WR024573, 2019.

Skiles, S. M., Painter, T. H., Deems, J. S., Bryant, A. C., and Landry, C. C.: Dust radiative forcing in snow of the Upper Colorado
590   River Basin: 2. Interannual variability in radiative forcing and snowmelt rates, 48, https://doi.org/10.1029/2012WR011986, 2012.

Skiles, S. M., Painter, T. H., Belnap, J., Holland, L., Reynolds, R. L., Goldstein, H. L., and Lin, J.: Regional variability in dust-on-snow processes and impacts in the Upper Colorado River Basin, 29, 5397–5413, https://doi.org/10.1002/hyp.10569, 2015.

Slater, A. G., Barrett, A. P., Clark, M. P., Lundquist, J. D., and Raleigh, M. S.: Uncertainty in seasonal snow reconstruction: Relative impacts of model forcing and image availability, Advances in Water Resources, 55, 165–177,
595   https://doi.org/10.1016/j.advwatres.2012.07.006, 2013.

Stewart, I. T.: Changes in snowpack and snowmelt runoff for key mountain regions, 23, 78–94, https://doi.org/10.1002/hyp.7128, 2009.

The Bureau of Reclamation: Emerging Technologies in Snow, 2022.

Trujillo, E. and Lehning, M.: Theoretical analysis of errors when estimating snow distribution through point measurements, 9,
600   1249–1264, https://doi.org/10.5194/tc-9-1249-2015, 2015.

Trujillo, E. and Molotch, N. P.: Snowpack regimes of the Western United States, 50, 5611–5623, https://doi.org/10.1002/2013WR014753, 2014.

Vernay, M., Lafaysse, M., Monteiro, D., Hagenmuller, P., Nheili, R., Samacoïts, R., Verfaillie, D., and Morin, S.: The S2M meteorological and snow cover reanalysis over the French mountainous areas, description and evaluation (1958–2020), 1–36,
605   https://doi.org/10.5194/essd-2021-249, 2021.

Winstral, A., Marks, D., and Gurney, R.: Assessing the Sensitivities of a Distributed Snow Model to Forcing Data Resolution, 15, 1366–1383, https://doi.org/10.1175/JHM-D-13-0169.1, 2014.